JOURNAL OF BACTERIOLOGY, Apr. 1994, p. 1850–1856
0021-9193/94/$04.00+0

Vol. 176, No. 7

Analysis of the Binding Site of the LysR-Type Transcriptional Activator TcbR on the *tcbR* and *tcbC* Divergent Promoter Sequences

JOHAN H. J. LEVEAU,[1] WILLEM M. DE VOS,[2] AND JAN ROELOF VAN DER MEER[1]*

Swiss Federal Institute for Environmental Science and Technology and Swiss Federal Institute for Technology, CH 8600 Dübendorf, Switzerland,[1] and Department of Microbiology, Wageningen Agricultural University, 6703 CT Wageningen, The Netherlands[2]

Received 19 October 1993/Accepted 12 January 1994

The TcbR transcriptional activator protein, which is encoded by the *tcbR* gene of *Pseudomonas* sp. strain P51 (J. R. van der Meer, A. C. J. Frijters, J. H. J. Leveau, R. I. L. Eggen, A. J. B. Zehnder, and W. M. de Vos, J. Bacteriol. 173:3700–3708, 1991), was purified from overproducing *Escherichia coli* cells by using a two-step chromatographic procedure. Subsequent use of TcbR in gel mobility shift assays with progressively shortened portions of a DNA fragment containing the divergent promoter sequences of the *tcbR* gene and the *tcbCDEF* operon showed that the direct binding site of TcbR is located between positions −85 to −40 relative to the *tcbCDEF* transcriptional start site, containing a LysR-type recognition sequence motif (T-N_{11}-A). DNase I footprinting experiments revealed that TcbR protected an area on both strands of the intercistronic region which was actually larger than this binding site (from positions −74 to −24). This stretch of protected DNA was interrupted by a region (positions −52 to −37) which became strongly hypersensitive to DNase I digestion upon addition of TcbR, suggesting that TcbR induces a bend in the DNA at this site.

Pseudomonas sp. strain P51 is able to use 1,2-dichlorobenzene, 1,4-dichlorobenzene, and 1,2,4-trichlorobenzene as sole carbon and energy sources (37, 38). The genes encoding the degradation of these compounds are located on catabolic plasmid pP51 and are organized in two gene clusters, *tcbAB* and *tcbCDEF* (35, 38). The expression of the *tcbCDEF* operon, which encodes the enzymes of a modified *ortho* cleavage pathway, is positively regulated by the gene product of *tcbR* (36). The *tcbR* gene is transcribed divergently from the *tcbC-DEF* operon and is located 160 bp upstream of *tcbC* (36). On the basis of amino acid sequence comparisons, the TcbR transcriptional activator protein was shown to belong to the LysR family (12, 13), which includes a number of other regulator proteins of aromatic degradation pathways, such as NahR (27, 28), CatR (18, 22, 23), ClcR (6), CatM (16), and TfdS (13, 14, 31). Gel mobility shift assay experiments revealed that the TcbR protein binds to DNA fragments that encompass the 160-bp region located between *tcbC* and *tcbR*, which contains the partially overlapping promoter sequences of both genes (36).

Here, we report (i) the purification of the TcbR protein from an overproducing *Escherichia coli* strain by using affinity and cation-exchange chromatography and (ii) an analysis of the interaction of TcbR with the *tcbC-tcbR* intercistronic region by using gel mobility shift assays and DNase I footprinting experiments.

MATERIALS AND METHODS

Bacterial strains, plasmids, and culture conditions. *E. coli* DH5α (25) was used for cloning experiments with plasmids. *E. coli* BL21(DE3) (32) harboring plasmid pLysS was used as the host strain for inducible overexpression of pET8c-derived plasmids (21). Plasmid pTCB77 (36) contains the intact *tcbR* gene under the control of the T7 φ10 promoter of pET8c and was used for overproduction of TcbR in *E. coli* BL21(DE3) cells. Plasmid pTCB77Δ is identical to pTCB77 except that it carries a frameshift mutation in the *tcbR* gene (36). Plasmid pTCB98 contains the *tcbC-tcbR* intercistronic region on a 0.22-kb *NcoI-MluI* fragment (Fig. 1), which was recovered from plasmid pTCB48 (38), filled in by using Klenow fragment of DNA polymerase I, and inserted into *SmaI*-digested pUC19 (41).

E. coli cultures were at 37°C grown on LB medium (25) supplemented with 50 μg of ampicillin per ml. For induction of *tcbR* in *E. coli*, isopropyl-β-D-thiogalactopyranoside (IPTG) was added to the medium at a concentration of 1 mM.

DNA manipulations and computer analyses. Plasmid DNA isolations, transformations and other DNA manipulations were carried out according to established procedures (25). Restriction enzymes and other DNA-modifying enzymes were obtained from Appligene (Illkirch, France), Life Technologies Inc. (Gaithersburg, Md.), or Pharmacia LKB Biotechnology (Uppsala, Sweden). Computer analyses of the primary sequence of TcbR were done with the Genetics Computer Group package (8).

Purification of TcbR. *E. coli* BL21(DE3)(pLysS) harboring plasmid pTCB77 was grown in 500 ml of LB to an optical density at 600 nm of 0.25 to 0.35. Cells were then induced by adding IPTG, and the culture was grown for another 4 h. Bacterial cells were harvested by centrifugation, washed once, recentrifuged, and finally resuspended in a lysis buffer containing 20 mM Tris-HCl (pH 7.5), 0.2 M NaCl, 5 mM $MgCl_2$, 1 mM dithiothreitol, 1 mM phenylmethylsulfonyl fluoride, and 1 μg of pancreatic DNase I (Fluka AG, Buchs, Switzerland) per ml. The cells were treated three times by immediate freezing in liquid nitrogen and heating in a water bath at 67°C and subsequently disrupted by three passages through a French pressure cell (Hypramag AG, Zürich, Switzerland) at 150 MPa. The suspension was centrifuged at 10,000 × *g* for 10 min

* Corresponding author. Mailing address: Department of Microbiology, EAWAG, Überlandstrasse 133, CH-8600 Duebendorf, Switzerland. Phone: + 41 1 823 5202. Fax: + 41 1 823 5028.

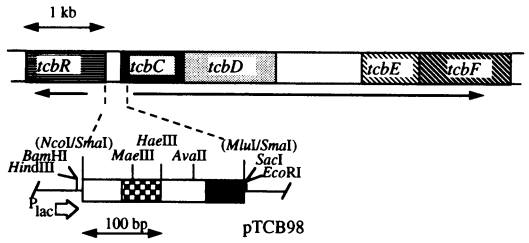

FIG. 1. Genetic organization of the *tcbCDEF* and *tcbR* operons and plasmid pTCB98, containing the 0.22-kb *Nco*I-*Mlu*I restriction fragment with the promoter regions of *tcbR* and *tcbCDEF*, which was used in this study. Hatches and shadings in the maps correspond to coding sequences of the *tcb* genes. The arrows underneath the maps indicate the direction of transcription. The checkerboard region in pTCB98 corresponds to the sequences at positions −25 to −75 from the transcriptional start site of *tcbC*, where the described interactions of TcbR with the DNA take place; horizontal bars represent *tcb* DNA; lines represent vector DNA. Relevant restriction sites are indicated, and those sites which were used for cloning but were modified during manipulation are shown within parentheses.

at 4°C, after which the supernatant was further cleared by centrifugation at 90,000 × *g* for 30 min at 4°C. The resulting supernatant was collected and is referred to as cell extract. Ten milligrams of protein was loaded onto a 6-ml heparin-Sepharose CL-6B (Pharmacia) bed packed in a 150-10 column (Merck), which was equilibrated with 20 mM Tris-HCl (pH 7.5)–0.2 M NaCl, operated at a flow rate of 0.75 ml/min. A Pharmacia LKB fast protein liquid chromatography system was used to run a linear salt gradient from 0.2 to 1.5 M NaCl in 20 mM Tris-HCl (pH 7.5). Fractions were collected, and the presence of TcbR was determined by analyzing the specific binding to a DNA fragment containing the promoter regions of *tcbC* and *tcbR* in a gel mobility shift assay as described earlier (36). TcbR protein eluted from the column at an NaCl concentration of 1.1 to 1.3 M. Fractions containing TcbR were pooled and desalted by centrifugation using Ultrafree-CL filters (10,000 nominal molecular weight limit; Millipore) to an NaCl concentration of 0.2 M. This preparation, referred to as partially purified TcbR, was loaded onto a 150-10 Fractogel EMD SO_3^--650 (S) column (Merck), which was equilibrated with 20 mM Tris-HCl (pH 7.5)–0.2 M NaCl, at a flow rate of 0.75 ml/min. TcbR protein was eluted by using a linear salt gradient from 0.2 to 2.0 M NaCl in 20 mM Tris-HCl (pH 7.5). The collected fractions were tested for the presence of TcbR as described above. TcbR protein eluted from this column at a salt concentration of approximately 1.8 M NaCl. TcbR-containing fractions were stored at 4°C until further use. This way of storage (high salt, 4°C) was found to be the most successful in minimizing losses in the DNA binding activity of TcbR. This preparation is referred to as purified TcbR. The degree of purification of TcbR protein after successive purification steps was estimated by determining the amount of total protein required to bind 50% of a radiolabeled specific DNA fragment (see above). The exact same growth conditions, cell extract preparation, and heparin-Sepharose purification procedure were performed with a culture of *E. coli* BL21(DE3)(pLysS) harboring plasmid pTCB77Δ. Heparin-Sepharose fractions with the same retention time as the TcbR-containing fractions in the purification procedure using *E. coli* BL21(DE3)(pLysS)(pTCB77) cell extracts were collected, stored at 4°C, and used as a negative control in subsequent experiments. This preparation is referred to as the TcbR negative control preparation.

Protein concentrations were determined with Coomassie brilliant blue G250 as described by Bradford (1). Bovine serum albumin (BSA) served as a protein standard.

Mapping of the TcbR binding site by using gel mobility shift DNA binding assays. A set of DNA probes used for the mapping of the TcbR binding site by gel mobility shift assays was generated as follows. Plasmid pTCB98 was digested with *Hin*dIII and *Eco*RI, and the 265-bp fragment containing the divergent promoters of *tcbC* and *tcbR* (Fig. 1) was isolated. This *Hin*dIII-*Eco*RI fragment was end labeled by using Klenow polymerase and [α-^{32}P]dATP (3,000 Ci/mmol; Amersham International plc, Amersham, United Kingdom). Progressively shortened fragments for binding were created by digesting the unlabeled *Hin*dIII-*Eco*RI fragment from pTCB98 with *Mae*III, *Hae*III, or *Ava*II, each having a single recognition site within this fragment at positions −58, −23, and +18, respectively, relative to the *tcbC* mRNA start site (Fig. 1). The resulting fragments were separated on a 2.0% agarose gel, isolated by using a Mermaid kit (Bio 101, Inc., La Jolla, Calif.), and end labeled by using Klenow polymerase. Two additional fragments were generated by enzymatic amplification (24) of pTCB98 template DNA with primers HindIII (5′-AGCTTG CATGCCTGCAGG-3′) and 930206 (5′-CAAATTAGTCA GCCATGC-3′) or with primers EcoRI (5′-AATTCGAGCT CGGTACCC-3′) and 930606 (5′-TGATGTGCCTATATTA CG-3′). Primers were labeled at the 5′ end by using T4 polynucleotide kinase and [γ-^{32}P]dATP (3,000 Ci/mmol; Amersham). Reaction mixtures contained, per 50 μl, 0.1 μg of each primer, 1 ng of pTCB98 DNA, 20 mM Tris-HCl (pH 8.4), 50 mM KCl, 2 mM $MgCl_2$, 0.05% W1 (Life Technologies, Inc.), 0.2 mM each deoxynucleoside triphosphate, 0.2 mg of BSA per ml, and 0.2 U of *Taq* polymerase. Amplification was carried out in a Crocodile II thermocycler (Appligene) in 30 cycles of 30 s at 93.5°C, 30 s at 54°C, and 45 s at 72°C, with a final extension of 4 min at 72°C. In this manner, DNA fragments containing the region from the *Hin*dIII site to the −40 position relative to the transcriptional start site of *tcbC* (primers HindIII and 930206) or containing the region from the −85 position to the *Eco*RI site (primers 930606 and EcoRI) were obtained. Labeled DNA fragments were then used in gel mobility shift assays with purified TcbR as described previously (36). In the text, the fragments are referred to as follows (numbers in parentheses indicate the left- and right-hand boundaries of the portion of the *tcbR-tcbC* intercistronic region contained on the fragment and are relative to the *tcbC* mRNA start site): *Hin*dIII-*Eco*RI; $F_{(-102/+114)}$; *Hin*dIII-*Ava*II, $F_{(-102/+18)}$; *Hin*dIII-*Hae*III, $F_{(-102/-23)}$; *Hin*dIII-930206, $F_{(-102/-40)}$; *Hin*dIII-*Mae*III, $F_{(-102/-58)}$; 930606-EcoRI, $F_{(-85/+114)}$; *Mae*III-*Eco*RI, $F_{(-58/+114)}$; *Hae*III-*Eco*RI, $F_{(-23/+114)}$; and *Ava*II-*Eco*RI, $F_{(+18/+114)}$.

DNase I footprinting analysis. DNase I footprinting was carried out on both strands of a DNA fragment containing the *tcbC-tcbR* intercistronic region. The bottom-strand labeled probe was generated by digestion of plasmid pTCB98 with *Hin*dIII, labeling at the 3′ end by using Klenow polymerase and [α-^{32}P]dATP, and a second digestion with *Eco*RI (Fig. 1). The labeled DNA restriction fragments were electrophoresed through agarose gel, and the 265-bp *Hin*dIII-*Eco*RI fragment was recovered by using a Geneclean kit. The top-strand probe was constructed by digesting plasmid pTCB98 with *Eco*RI, labeling with Klenow polymerase, a second digestion with *Bam*HI, and recovery of the fragment (Fig. 1). For DNase I footprinting experiments, the procedure of de Lorenzo et al. (7) was used. Labeled DNA fragments were preincubated for 3 min at 30°C with various amounts of TcbR protein or TcbR negative control preparation in a final volume of 100 μl of

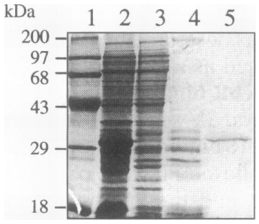

FIG. 2. Purification of the TcbR protein, as shown by SDS-polyacrylamide gel electrophoresis analysis of protein extracts during the various stages of the purification procedure. Lanes: 1, protein mass markers; 2, total extract of *E. coli* BL21(DE3) cells harboring plasmid pTCB77; 3, cell extract of *E. coli* BL21(DE3)(pTCB77); 4, heparin-Sepharose fraction showing TcbR-mediated DNA binding activity; 5, protein fraction after SO_3^- cation-exchange column purification showing TcbR-mediated DNA binding activity.

solution containing 20 mM Tris-HCl (pH 7.5), 2 mM $MgCl_2$, 1 mM $CaCl_2$, 0.1 mM EDTA, 40 mM KCl, 100 μg of BSA per ml, and 20 μg of poly(dI-dC) (Boehringer, Mannheim, Germany) per ml. As source for active TcbR protein in these experiments, we used purified TcbR or the partially purified TcbR preparation. To control the effect of a few contaminating proteins present in the partially purified TcbR preparation, we also included the TcbR negative control. Subsequently, 0.06 U of RNase-free DNase I (Boehringer) was added to the mixture. The digestion was allowed to proceed for exactly 2 min at 30°C, after which 50 μl of stop buffer (0.1 M EDTA [pH 8.0], 0.8% sodium dodecyl sulfate [SDS], 1.6 M ammonium acetate, 300 μg of tRNA from brewer's yeast [Boehringer] per ml) was added. Nucleic acids were precipitated, dried, and dissolved in 2.5 μl of loading buffer (95% formamide, 20 mM EDTA, 0.05% bromophenol blue, 0.05% xylene cyanol). Samples were then heated for 2 min at 80°C and loaded on a DNA sequencing gel. As a size marker for the DNase I footprints, a Sanger sequencing ladder (26) was generated, using plasmid pTCB98 and primers HindIII or EcoRI (see above), which match the beginning of the fragments used for the footprint analysis. The autoradiograms were quantitatively analyzed by densitometry scanning (300S computing densitometer; Molecular Dynamics, Sunnyvale, Calif.), using the program ImageQuant (Molecular Dynamics). For each band in the DNase I digestion pattern, the absolute density on the autoradiogram was determined. Relative density values were then computed by dividing densities of bands in the reactions with TcbR protein by those of the corresponding bands in the control DNase I digestion.

RESULTS

Purification of the TcbR protein. Plasmid pTCB77, containing the *tcbR* gene fused with the ATG codon of pET8c behind the T7 ϕ10 promoter, was previously used to analyze *tcbR* expression in *E. coli* (36). High levels of TcbR production were obtained in *E. coli* BL21(DE3)(pTCB77) upon induction with IPTG (Fig. 2, lane 2). Most of the TcbR protein, however, was in an insoluble form. Cell extracts prepared from these cells after induction (Fig. 2, lane 3) were used for the purification of TcbR. The property of TcbR to bind DNA was exploited in the purification procedure by using affinity chromatography on a heparin-Sepharose column. TcbR eluted from the column at an NaCl concentration of about 1.2 M, which indicates a high affinity of the TcbR protein for the ligand heparin. This step resulted in an approximate 500-fold purification of TcbR, as estimated from gel mobility shift assays as well as from protein gels (Fig. 2, lane 4). As a second purification step, cation-exchange chromatography was applied. This resulted in a high-level purification of TcbR, which eluted at an NaCl concentration of approximately 1.8 M. The purity of TcbR was estimated to be over 90%, as judged from Coomassie brilliant blue-stained SDS-polyacrylamide gels (Fig. 2, lane 5). A TcbR negative control sample was prepared by performing the exact same purification steps with cell extracts of *E. coli* BL21 (DE3)(pTCB77Δ). This strain produced a truncated TcbR protein with a size of about 12 kDa, which was unable to bind the *tcbC-tcbR* intercistronic region, as reported previously (36). Protein fractions were collected after purification on heparin-Sepharose and appeared to contain similar contaminating proteins as purified TcbR after the heparin-Sepharose step but lacked the 32-kDa TcbR protein. We could not detect any binding activity of 77Δ protein fractions in gel mobility shift assays with the *tcbC-tcbR* operator DNA fragment (results not shown). These purified protein samples served as a negative control in DNA binding and bending experiments.

Mapping of the TcbR binding site in a gel mobility shift assay. In a previous study (36), it was shown that the TcbR protein binds specifically to a 360-bp DNA fragment containing the *tcbC-tcbR* intercistronic region. To determine more precisely the TcbR binding site on this DNA fragment, a series of overlapping deletion fragments was generated and tested for the ability to be bound by TcbR (Fig. 3A). The right-hand boundary of the TcbR binding site was determined with fragments decreasing in length starting from the *Eco*RI site (Fig. 3B). We found that fragments $F_{(-102/+114)}$, $F_{(-102/+18)}$, $F_{(-102/-23)}$, and $F_{(-102/-40)}$ all retained the ability to be bound by TcbR; however, no binding was observed with fragment $F_{(-102/-58)}$ (Fig. 3B). From these observations we concluded that sequences upstream from position −40 within the −102 to +114 region of the *tcbC* promoter are necessary for binding by TcbR. The left-hand boundary was determined in a similar manner by using fragments that were sequentially shortened from the *Hin*dIII site. Whereas fragment $F_{(-85/+114)}$ was bound by TcbR, fragments $F_{(-58/+114)}$, $F_{(-23/+114)}$, and $F_{(+18/+114)}$ all had lost the ability to be bound by TcbR protein (Fig. 3C). This result showed that the sequences necessary for binding by TcbR were downstream from position −85. The binding site of the TcbR protein on its operator DNA therefore appeared to be located between positions −85 and −40 relative to the *tcbC* transcriptional start site. Interestingly, digesting at the *Mae*III site, which prevented TcbR binding, disrupted a 5-bp hyphenated inverted repeat sequence (TTACG CAAAC CGTAA; nucleotides −71 to −58) that we think may be important for the recognition and binding of TcbR (see below).

DNase I footprinting analysis. To obtain further information on the interaction of the TcbR protein with the *tcbR-tcbC* operator region, we performed a DNase I footprinting analysis. For this purpose, the operator region was recovered as the 265-bp *Hin*dIII-*Eco*RI fragment from plasmid pTCB98 (Fig. 1). Both top and bottom strands of this fragment were analyzed for TcbR protection. When the top-strand labeled DNA was incubated with DNase I and TcbR protein, a region of protection from DNase I digestion that ranged from nucleotides −74 to −17 relative to the *tcbC* transcription start site was found (Fig. 4A, lane 4). This region was not protected in footprinting reactions to which the TcbR negative control preparation was added (Fig. 4A, lane 3), confirming the active role of TcbR in the observed DNA-protein interactions. This result showed that TcbR apparently interacts with a larger region on the operator DNA than required for binding itself (see above). At positions −47 through −50, strong DNase

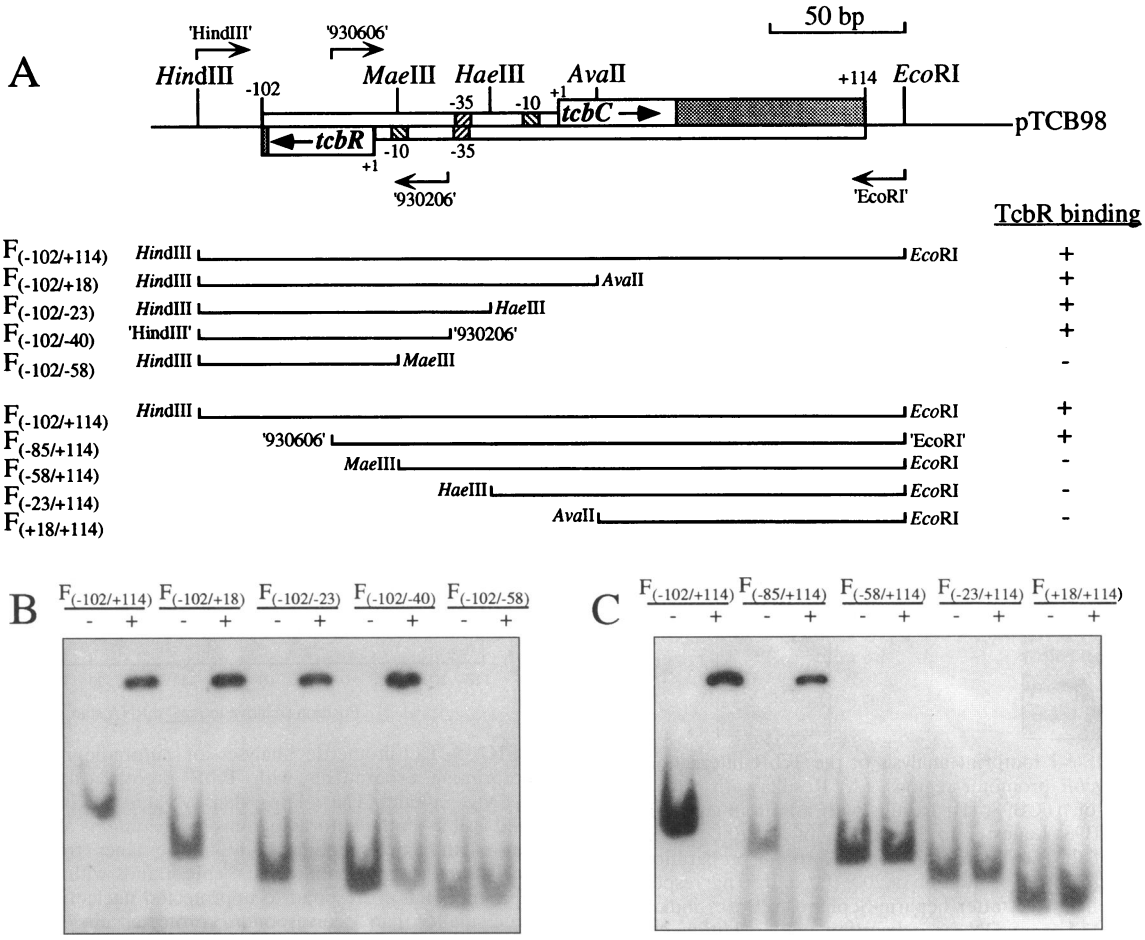

FIG. 3. Mapping of the TcbR binding site by using gel mobility shift assays. (A) Schematic representation of plasmid pTCB98, containing the *tcbR-tcbC* intercistronic region, and the deletion fragments that were used in gel mobility shift assays to determine the boundaries of the TcbR binding site. The mRNA start sites, as well as the −35 and −10 boxes of both *tcbR* and *tcbC*, are indicated. The coding regions of both genes are shaded. Positions of relevant restriction sites, as well as the orientations of primers HindIII, EcoRI, 930206, and 930606 (see Materials and Methods), are shown. The fragments used in the gel mobility shift assays are drawn below. The numbers in parentheses indicate the left- and right-hand boundaries of the portion of the *tcbR-tcbC* intercistronic region contained on the fragment and are relative to the *tcbC* mRNA start site. The ability (+) or inability (−) of the DNA deletion fragments to be bound by TcbR is indicated on the right. (B) Autoradiogram of the results of the gel mobility shift assays using different deletion fragments shortened from the *Eco*RI site. (C) Gel mobility shifts using fragments shortened from the *Hin*dIII site. Symbols: −, no TcbR added; +, addition of 20 ng of TcbR protein extract after heparin-Sepharose.

I-hypersensitive sites were observed in the presence of TcbR, while weaker DNase I-hypersensitive sites were found at positions −37 and −38. DNase I footprinting of the bottom-strand labeled probe revealed a TcbR-protected region that ranged from nucleotides −81 to −24 (Fig. 4B, lane 4), with strong hypersensitive sites at positions −39, −40, −51, and −52 and weaker ones at positions −41, −42, −44, and −45. A quantitative analysis of the autoradiograms of several DNase I footprinting experiments with purified TcbR by scanning densitometry confirmed that protection of both strands against DNase I digestion in the presence of TcbR occurred at two distinct regions, i.e., from −74 to −56 and from −34 to −24 (Fig. 5). Addition of increasing amounts of TcbR to the DNase I footprinting reaction of the top strand resulted in a uniformly increasing protection of both of these regions (Fig. 5). For the bottom strand, however, protection of the region from −34 to −24 seemed to increase at a slower rate with increasing TcbR amounts than was the case with the region from −74 to −56. An overview of the TcbR-mediated contacts on the operator DNA is given in Fig. 6.

DISCUSSION

Expression of the chlorocatechol oxidative operon in *Pseudomonas* sp. strain P51 is positively regulated by the gene product of *tcbR*, a LysR-type transcriptional activator (36). In this study, we describe the purification of TcbR protein from cell extracts of an overproducing *E. coli* strain. We observed that most of the produced TcbR protein in *E. coli* formed insoluble aggregates, from which no active TcbR could be recovered. However, from the fraction which remained soluble in *E. coli*, we could isolate and purify TcbR protein to apparent homogeneity by applying a two-step chromatographic procedure. In the course of purification, it was observed that the TcbR protein has a high affinity for negatively charged molecules such as heparin and SO_3^-. This property may reflect the

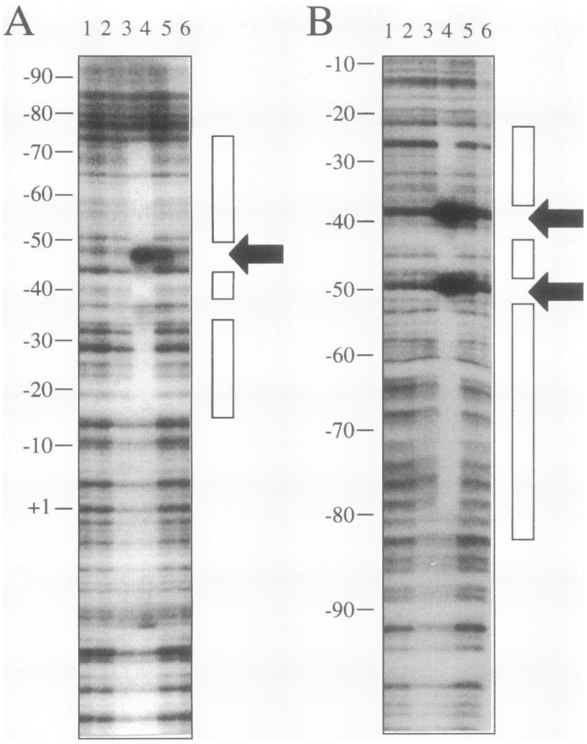

FIG. 4. DNase I footprint analysis of the TcbR interactions with the *tcbC* and *tcbR* promoter regions. (A) Results with a top-strand labeled probe of pTCB98. (B) Results with a bottom-strand labeled probe of pTCB98. Lanes: 1 to 3, addition of 50, 100, and 200 ng, respectively, of the TcbR negative control protein preparation after heparin-Sepharose; 4 to 6, addition of 200, 100, and 50 ng, respectively, of TcbR protein extract after heparin-Sepharose. Boxes indicate the regions protected from DNase I digestion upon addition of TcbR protein extract. Arrows indicate regions of strong DNase I-hypersensitive sites. Numbers at the left indicate nucleotide positions relative to the *tcbC* transcriptional start site.

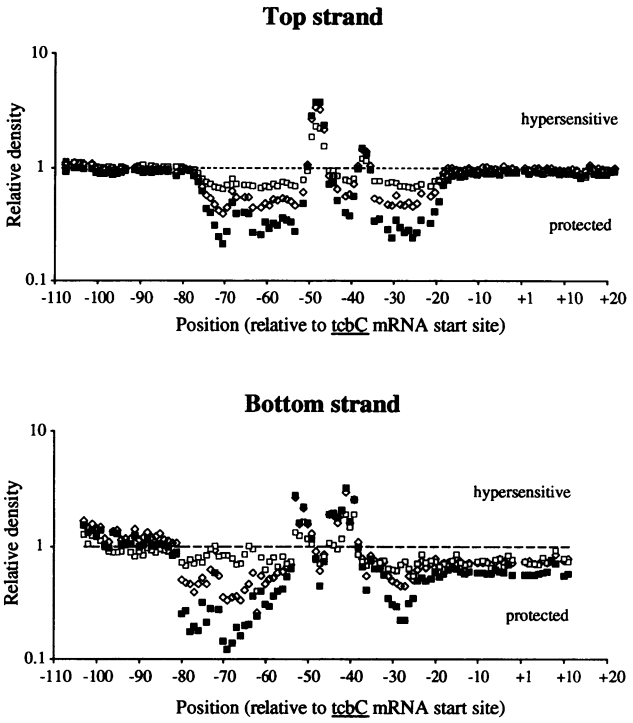

FIG. 5. Densitometric analyses of autoradiograms of DNase I footprinting experiments with TcbR protein extract after cation-exchange column. The relative density value was calculated for each band visible on the autoradiograms by dividing its absolute density by that of the corresponding band in the lanes from the DNase I incubations without addition of TcbR. Bands with a relative density value of 1 thus correspond to unprotected nucleotides, bands with a value smaller than 1 correspond to protected nucleotides, and bands with a value higher than 1 correspond to hypersensitive sites. Symbols: □, 12 ng of TcbR protein added; ◇, 30 ng of TcbR added; ■, 60 ng of TcbR added.

unusually high pI of 10.5 of TcbR as calculated by computer analysis (8).

To determine the location of the TcbR binding site on its operator DNA, a bidirectional set of progressively shortened DNA fragments was constructed and tested for the ability to be bound by TcbR in gel mobility shift assays. These experiments indicated that the region from −85 to −40 relative to the *tcbC* mRNA start site is necessary for binding by TcbR. Interestingly, in DNase I footprinting experiments, we observed that the interaction between TcbR and the *tcbC-tcbR* operator region was actually larger (i.e., from positions −74 to −24) (Fig. 6). Footprints of similar size were reported for other LysR transcriptional activators, such as NodD (9), OccR (39), and OxyR (5, 30) (55, 50, and 45 bp, respectively). It appears that the protein-DNA interactions which we found for TcbR are almost identical to those reported for OccR (39). In the first place, in the absence of inducer (which for OccR expression is octopine) (39), OccR and TcbR protect approximately 50 bp on both strands of the DNA, i.e., from positions −74 to −23 and −74 to −24, respectively. Furthermore, similarly located DNase I-hypersensitive sites were found in regions from −52 to −36 and −52 to −37, respectively. Interestingly, the spacing of these sites on top and bottom strands indicates that they are all located on one side of the DNA helix (Fig. 5 and 6). They may have become hypersensitive for DNase I digestion as a result of a strong bending of the DNA in that region. It was shown that OccR mediates such a local bend in the DNA around position −50 in the absence of its inducer (39). Preliminary results of experiments which assessed the amounts of intramolecular ligation product (19) formed from a DNA fragment containing the *tcb* operator region in the presence of TcbR suggest that TcbR may induce a bend on the DNA (34). Unfortunately, possible TcbR-induced bending could not be observed in a circular permutation assay (such as were used to demonstrate DNA bending by OccR or RepA) (19, 39). Possibly because of the high isoelectric point of the TcbR protein, DNA-TcbR complexes do not migrate efficiently into polyacrylamide gels, making it impossible to observe differences in mobilities of these complexes caused by DNA bending.

Characteristic for most LysR-type binding sites is a T-N_{11}-A motif, generally located 50 to 60 bp upstream from the transcription start site of the regulated gene (11). This motif is likely to contain the nucleotides which provide the contacts with the proposed helix-turn-helix domain in the N-terminal end of LysR-type proteins (12, 13, 36). Other procaryotic DNA binding proteins with helix-turn-helix domains similarly bind sequences with hyphenated dyad symmetry (17, 29). The TcbR protected region contains such a LysR motif, which is part of a 5-bp hyphenated perfect inverted repeat sequence (T-$_{-72}$ TACG CAAAC CGTAA-$_{-58}$) (Fig. 6). The spacing of 5

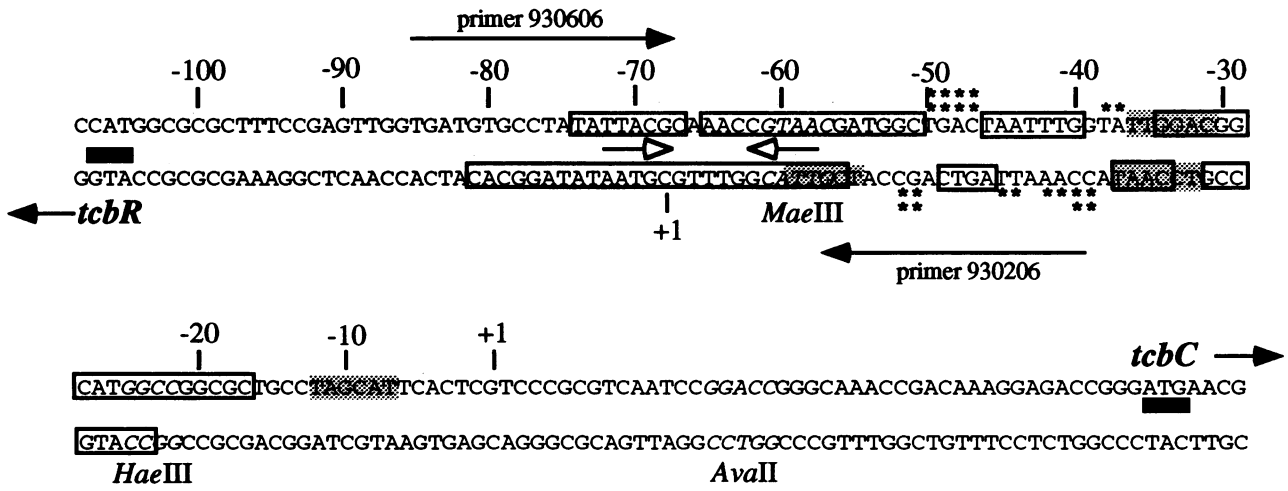

FIG. 6. Overview of the interactions of TcbR on the intercistronic regions of *tcbR* and *tcbC*. Numbers above the DNA sequence indicate positions relative to the transcriptional start site (+1) of *tcbC*. Also indicated is the transcriptional start site of *tcbR*. The −10 and −35 boxes of both genes are shaded; the ATG start codons of both genes are indicated by black bars. The regions protected from DNase I digestion by TcbR on each strand are boxed. Asterisks show strong (**) and weak (*) hypersensitive sites. The 5-bp hyphenated inverted repeat forming the putative center of TcbR binding is indicated by open arrows. Recognition sites of the endonucleases used for the deletion analysis (see Fig. 3A) are indicated in italics on the sequence. Also shown are the locations of primers 930206 and 930606.

nucleotides would place the two 5-bp repeats in adjacent grooves on one face of the DNA double helix, providing contacts for binding by a putative TcbR dimer.

It is at present still unclear what the mode of action of LysR regulators upon induction is and whether there is a single manner used by all. Although in all LysR-type systems studied so far, protein-DNA binding takes place under both uninduced and induced conditions, subtle differences appear to exist in the protein-DNA interactions. For instance, upstream sequences of LysR-type regulated promoters can contain more than one LysR binding motif, e.g., as reported for NodD (9) and IlvY (40). Results from mutation analysis suggest that two NodD protein molecules occupy two adjacent binding motifs under both uninduced and induced conditions (9). Other LysR-type regulators, such as TrpI and CatR, protect under uninduced conditions a relatively small region on the DNA containing a single LysR motif sequence (3, 18). However, in the presence of an inducer molecule, the binding affinity of TrpI and CatR for their target DNA increased severalfold (4, 18). Furthermore, the presence of an effector seemed to result in cooperative binding of additional protein molecules to the DNA. A third type of LysR regulators, exemplified by AmpR (15), MetR (2, 33), and OccR (39), appears to bind to a single site on the target DNA. Our results favor a model of TcbR binding which is similar to that of OccR (39). TcbR and OccR (39) both interact with an additional region (for TcbR, the area from −34 to −24) outside their direct binding sites (−74 to −54 for TcbR) (Fig. 4 to 6). This area alone is not sufficient for binding by TcbR, as was revealed by our footprinting studies and gel mobility shift assays. Interactions of TcbR with this area could be the result of an induced bend in the DNA downstream of the direct binding site. It is presently unclear whether the interaction with this region takes place with the TcbR protein molecules that occupy the direct binding site or by cooperative binding of additional TcbR molecules. Studies with the TcbR system are presently hampered in particular by the nature of the possible inducer molecules (e.g., chlorinated muconic acids). We tested the effect of addition of 3-chlorocatechol and 2-chloromuconic acid at a final concentration of 1 μM on DNA binding by TcbR. However, at these concentrations, no differences in DNase I footprints or affinity for DNA binding were detected (results not shown).

Of particular interest to the study of the TcbR system are two other described chlorocatechol oxidative operons, i.e., *clcABD* from *Pseudomonas putida* (10) and *tfdCDEF* from *Alcaligenes eutrophus* JMP134 (20), which were also proposed to be regulated by a LysR-type transcriptional activator (6, 13). Extensive sequence identity exists between the operator sequence of the *tcbCDEF* operon and upstream sequences of the *clcABD* and *tfdCDEF* clusters, i.e., in the −10 and −35 promoter boxes (36) and in areas of the *clc* and *tfd* sequences corresponding to the operator region of *tcbC* from −72 to −58 (not shown). Here, similar 5-bp hyphenated inverted repeats containing the T-N_{11}-A LysR motif can be found (6). As previously reported, TcbR protein shows cross-binding in vitro to a DNA fragment containing the upstream region of the *tfdCDEF* operon, which indicates the high degree of similarity between these two regulatory systems (36). Further analysis of the details of regulation in closely related degradation pathways of aromatic compounds (6, 16, 18, 22, 23, 28, 36) will be very useful for obtaining more information on the mechanisms of their evolutionary divergence and specialization.

REFERENCES

1. **Bradford, M. M.** 1976. A rapid and sensitive method for the quantification of microgram quantities of protein utilizing the principle of protein-dye binding. Anal. Biochem. **72**:248–254.
2. **Byerly, K. A., M. L. Urbanowski, and G. V. Stauffer.** 1991. The MetR binding site in the *Salmonella typhimurium metH* gene: DNA sequence constraints on activation. J. Bacteriol. **173**:3547–3553.
3. **Chang, M., and I. P. Crawford.** 1990. The roles of indoleglycerol phosphate and the TrpI protein in the expression of *trpBA* from *Pseudomonas aeruginosa*. Nucleic Acids Res. **18**:979–988.
4. **Chang, M., and I. P. Crawford.** 1991. In vitro determination of the effect of indoleglycerol phosphate on the interaction of purified TrpI protein with its DNA-binding sites. J. Bacteriol. **173**:1590–1597.
5. **Christman, M. F., G. Storz, and B. N. Ames.** 1989. OxyR, a positive regulator of hydrogen peroxide-inducible genes in *Esch-*

erichia coli and *Salmonella typhimurium*, is homologous to a family of bacterial regulatory proteins. Proc. Natl. Acad. Sci. USA **86**:3484–3488.

6. **Coco, W. M., R. K. Rothmel, S. Henikoff, and A. M. Chakrabarty.** 1993. Nucleotide sequence and initial functional characterization of the *clcR* gene encoding a LysR family activator of the *clcABD* chlorocatechol operon in *Pseudomonas putida*. J. Bacteriol. **175:** 417–427.
7. **de Lorenzo, V., M. Herrero, M. Metzke, and K. N. Timmis.** 1991. An upstream XylR- and IHF-induced nucleoprotein complex regulates the σ^{54}-dependent Pu promoter of TOL plasmid. EMBO J. **10**:1159–1169.
8. **Devereux, J., P. Haeberli, and O. Smithies.** 1984. A comprehensive set of sequence analysis programs for the VAX. Nucleic Acids Res. **12**:387–395.
9. **Fisher, R. F., and S. R. Long.** 1989. DNA footprint analysis of the transcriptional activator proteins NodD1 and NodD3 on inducible *nod* gene promoters. J. Bacteriol. **171**:5492–5502.
10. **Frantz, B., and A. M. Chakrabarty.** 1987. Organization and nucleotide sequence determination of a gene cluster involved in 3-chlorocatechol degradation. Proc. Natl. Acad. Sci. USA **84:** 4460–4464.
11. **Goethals, K., M. van Montagu, and M. Holsters.** 1992. Conserved motifs in a divergent *nod* box of *Azorhizobium caulinodans* ORS571 reveal a common structure in promoters regulated by LysR-type proteins. Proc. Natl. Acad. Sci. USA **89**:1646–1650.
12. **Henikoff, S., G. W. Haughn, J. M. Calvo, and J. C. Wallace.** 1988. A large family of bacterial activator proteins. Proc. Natl. Acad. Sci. USA **85**:6602–6606.
13. **Henikoff, S., J. C. Wallace, and J. P. Brown.** 1990. Finding protein similarities with nucleotide sequence databases. Methods Enzymol. **183**:111–133.
14. **Kaphammer, B., and R. H. Olsen.** 1990. Cloning and characterization of *tfdS*, the repressor-activator gene of *tfdB*, from the 2,4-dichlorophenoxyacetic acid catabolic plasmid pJP4. J. Bacteriol. **172**:5856–5862.
15. **Lindquist, S., F. Lindberg, and S. Normark.** 1989. Binding of the *Citrobacter freundii* AmpR regulator to a single DNA site provides both autoregulation and activation of the inducible *ampC* β-lactamase gene. J. Bacteriol. **171**:3746–3753.
16. **Neidle, E. L., C. Hartnett, and L. N. Ornston.** 1989. Characterization of *Acinetobacter calcoaceticus catM*, a repressor gene homologous in sequence to transcriptional activator genes. J. Bacteriol. **171**:5410–5421.
17. **Pabo, C. O., and R. T. Sauer.** 1984. Protein-DNA recognition. Annu. Rev. Biochem. **53**:293–321.
18. **Parsek, M. R., D. L. Shinabarger, R. K. Rothmel, and A. M. Chakrabarty.** 1992. Roles of CatR and *cis,cis*-muconate in activation of the *catBC* operon, which is involved in benzoate degradation in *Pseudomonas putida*. J. Bacteriol. **174**:7798–7806.
19. **Pérez-Martin, J., and M. Espinosa.** 1991. The RepA repressor can act as a transcriptional activator by inducing DNA bends. EMBO J. **10**:1375–1382.
20. **Perkins, E. J., M. P. Gordon, O. Caceres, and P. F. Lurquin.** 1990. Organization and sequence analysis of the 2,4-dichlorophenol hydroxylase and dichlorocatechol oxidative operons of plasmid pJP4. J. Bacteriol. **172**:2351–2359.
21. **Rosenberg, A. H., B. N. Lade, D.-S. Chui, S.-W. Lin, J. J. Dunn, and F. W. Studier.** 1987. Vectors for selective expression of cloned DNAs by T7 RNA polymerase. Gene **56**:125–135.
22. **Rothmel, R. K., T. L. Aldrich, J. E. Houghton, W. M. Coco, L. N. Ornston, and A. M. Chakrabarty.** 1990. Nucleotide sequencing and characterization of *Pseudomonas putida catR*: a positive regulator of the *catBC* operon is a member of the LysR family. J. Bacteriol. **172**:922–931.
23. **Rothmel, R. K., D. L. Shinabarger, M. R. Parsek, T. L. Aldrich, and A. M. Chakrabarty.** 1991. Functional analysis of the *Pseudomonas putida* regulatory protein CatR: transcriptional studies and determination of the CatR DNA-binding site by hydroxyl-radical footprinting. J. Bacteriol. **173**:4717–4724.
24. **Saiki, R. K., D. H. Gelfand, S. Stoffel, S. J. Scharf, R. Higuchi, G. T. Horn, K. B. Mullis, and H. E. Erlich.** 1988. Primer-directed enzymatic amplification of DNA with a thermostable DNA polymerase. Science **239**:487–491.
25. **Sambrook, J., E. F. Fritsch, and T. Maniatis.** 1989. Molecular cloning: a laboratory manual, 2nd ed. Cold Spring Harbor Laboratory, Cold Spring Harbor, N.Y.
26. **Sanger, F. S., S. Nicklen, and A. R. Coulson.** 1977. DNA sequencing with chain-terminating inhibitors. Proc. Natl. Acad. Sci. USA **74**:5463–5467.
27. **Schell, M. A., and E. Poser.** 1989. Demonstration, characterization, and mutational analysis of NahR protein binding in *nah* and *sal* promoters. J. Bacteriol. **171**:837–846.
28. **Schell, M. A., and M. Sukordhaman.** 1989. Evidence that the transcription activator encoded by the *Pseudomonas putida nahR* gene is evolutionarily related to the transcription activators encoded by the *Rhizobium nodD* genes. J. Bacteriol. **171**:1952–1959.
29. **Schleif, R.** 1988. DNA binding by proteins. Science **241**:1182–1187.
30. **Storz, G., L. A. Tartaglia, and B. N. Ames.** 1990. Transcriptional regulator of oxidative stess-inducible genes: direct activation by oxidation. Science **248**:189–194.
31. **Streber, W. R., K. N. Timmis, and M. H. Zenk.** 1987. Analysis, cloning, and high-level expression of 2,4-dichlorophenoxyacetate monooxygenase gene *tfdA* of *Alcaligenes eutrophus*. J. Bacteriol. **169**:2950–2955.
32. **Studier, F. W., and B. A. Moffatt.** 1986. Use of bacteriophage T7 RNA polymerase to direct selective high-level expression of cloned genes. J. Mol. Biol. **189**:113–120.
33. **Urbanowski, M. L., and G. V. Stauffer.** 1989. Genetic and biochemical analysis of the MetR activator-binding site in the *metE metR* control region of *Salmonella typhimurium*. J. Bacteriol. **171**:5620–5629.
34. **van der Meer, J. R.** Unpublished results.
35. **van der Meer, J. R., R. I. L. Eggen, A. J. B. Zehnder, and W. M. de Vos.** 1991. Sequence analysis of the *Pseudomonas* sp. strain P51 *tcb* gene cluster, which encodes metabolism of chlorinated catechols: evidence for specialization of catechol 1,2-dioxygenases for chlorinated substrates. J. Bacteriol. **173**:2425–2434.
36. **van der Meer, J. R., A. C. J. Frijters, J. H. J. Leveau, R. I. L. Eggen, A. J. B. Zehnder, and W. M. de Vos.** 1991. Characterization of the *Pseudomonas* sp. strain P51 gene *tcbR*, a LysR-type transcriptional activator of the *tcbCDEF* chlorocatechol oxidative operon, and analysis of the regulatory region. J. Bacteriol. **173**:3700–3708.
37. **van der Meer, J. R., W. Roelofsen, G. Schraa, and A. J. B. Zehnder.** 1987. Degradation of low concentrations of dichlorobenzenes and 1,2,4-trichlorobenzene by *Pseudomonas* sp. strain P51 in nonsterile soil columns. FEMS Microbiol. Ecol. **45**:333–341.
38. **van der Meer, J. R., A. R. W. van Neerven, E. J. de Vries, W. M. de Vos, and A. J. B. Zehnder.** 1991. Cloning and characterization of plasmid-encoded genes for the degradation of 1,2-dichloro-, 1,4-dichloro-, and 1,2,4-trichlorobenzene of *Pseudomonas* sp. strain P51. J. Bacteriol. **173**:6–15.
39. **Wang, L., J. D. Helmann, and S. C. Winans.** 1992. The *A. tumefaciens* transcriptional activator OccR causes a bend at a target promoter, which is partially relaxed by a plant tumor metabolite. Cell **69**:659–667.
40. **Wek, R. C., and G. W. Hatfield.** 1988. Transcriptional activation at adjacent operators in the divergent-overlapping *ilvY* and *ilvC* promoters of *Escherichia coli*. J. Mol. Biol. **203**:643–663.
41. **Yanisch-Perron, C., J. Vieira, and J. Messing.** 1985. Improved M13 phage cloning vectors and host strains: nucleotide sequences of the M13mp18 and pUC19 vectors. Gene **33**:103–119.